

Synthesis, Characterization and Crystal Structure of *trans*-[2,6-Bis(3-phenylpyrazol-1-yl- κN^2)pyridine- κN]chloro-bis(trimethylphosphine)ruthenium(II) Perchlorate: Evidence for Meridional Steric Crowding †

Carol A. Bessel,^a Ronald F. See,^a Donald L. Jameson,^b Melvyn Rowen Churchill^{*.a} and Kenneth J. Takeuchi^{*.a}

^a Department of Chemistry, State University of New York at Buffalo, Buffalo, New York 14214, USA

^b Department of Chemistry, Gettysburg College, Gettysburg, PA, 17325-1486, USA

The synthesis, characterization, and crystal structure of *trans*-[RuL(Cl)(PMe₃)₂]ClO₄ [L = 2,6-bis(3-phenylpyrazol-1-yl)pyridine] are reported. The complex crystallizes in the non-centrosymmetric trigonal space group *P*3₁21 (no. 152) with *a* = 14.158(2), *c* = 14.493(3) Å, and *Z* = 3. Both the Ru^{II}-containing cation and the perchlorate anion (which is disordered) lie on a crystallographic two-fold axis. This represents the first structural characterization of a transition-metal complex which utilizes a member of the family of bis(pyrazolyl)pyridine ligands. In addition, the crystal structure yields evidence that the ligand L may be sterically more suitable for co-ordination to a ruthenium(II) centre than the analogous diphenyl-substituted terpyridine ligand, dpt (6,6''-diphenyl-2,2':6',2''-terpyridine). For both tridentate ligands, the donor nitrogen atoms take up three meridional sites and the phenyl substituents are directed toward the fourth equatorial co-ordination site; however, due to the large distance between the two phenyl arms of L (relative to the dpt), the former ligand can be utilized in synthesising the present ruthenium(II) complex whereas the analogous dpt complex cannot readily be prepared.

The introduction of sterically hindering or directing substituents onto multidentate nitrogen donor ligands may have long-range consequences on the reactivity of many of the transition-metal complexes which utilize such ligands.¹⁻⁹ For example, recent work with Cu(dpphen) (dpphen = 2,9-diphenyl-1,10-phenanthroline) complexes has shown that the phenyl substituents of dpphen significantly influence the manner in which the copper complex binds to DNA as well as influencing the excited-state lifetimes.¹⁰ In addition, complexes of Rh and Ir which incorporate dmphen (2,9-dimethyl-1,10-phenanthroline) have been proven to be efficient water gas shift catalysts^{11a} while *cis*-[Ru^{VI}(dmphen)₂O₂][PF₆]₂ has been studied in the oxidation of organic substrates.^{11b} Similarly, bipy (2,2'-bipyridine) ligands have been extensively modified synthetically.¹² Ruthenium co-ordination complexes utilizing the bipy and substituted bipy ligands have been studied in relation to their remarkable reactivity which is manifested in the photoproduction of H₂ and O₂ from H₂O and their use in photochemical cells to convert and store solar energy.¹³

Investigations of the structural effects caused by the 6,6'' disubstitution of terpy (2,2':6',2''-terpyridine) ligands on transition-metal complex reactivity are relatively rare.^{14,15} Although ruthenium complexes which utilize terpy ligands have been proven catalytically to oxidize water to molecular oxygen^{8,16} and to act as oxygen-atom transfer agents for the oxidation of benzyl alcohol and norbornene,^{17,18} there have been no crystallographic structural determinations of 6,6''-disubstituted terpy ligands which are co-ordinated to ruthenium in a tridentate fashion. This may be due to the synthetic difficulty of structurally modifying the ligands in such a way as to maintain the tridentate character without the formation of bimetallic systems.^{14,15,19}

The ability sterically to constrain the access of a substrate to an active transition-metal centre has been proposed to be of importance in the development of substrate-specific catalysts.¹¹ Our work with Ru^{III}(terpy)(NO₂) complexes which are capable of acting as oxygen-transfer agents^{17,18} led us to investigate the dpt (6,6''-diphenyl-2,2':6',2''-terpyridine) ligand (prepared in overall 20% yield)^{19b} as a possible means of sterically controlling access to the nitro ligand. However, although we employed a variety of synthetic routes and a number of different ruthenium starting materials, e.g. RuCl₃·3H₂O, [RuCl₂(dmsO)₄] (dmsO = dimethyl sulphoxide) and K₂[Ru(OH₂)Cl₅], we were unable to synthesize *trans*-[RuCl₂(dpt)(PMe₃)₂], an intermediate material in the multistep synthesis of nitroruthenium(III) complexes. From this set-back we became interested in investigating the steric limitations regarding the co-ordination of sterically crowded ligands to a ruthenium(II) centre. Thus, we synthesised a new ligand, 2,6-bis(3-phenylpyrazol-1-yl)pyridine (L),⁹ which is structurally similar to dpt, and we were successful in the synthesis of *trans*-[RuL(Cl)(PMe₃)₂]ClO₄, the immediate precursor to the nitroruthenium complex. We have also determined its crystal structure, the first of a transition-metal complex which utilizes a member of the bis(pyrazolyl)pyridine ligand family. The structural data obtained can be utilized to rationalize the synthetic difficulties associated with dpt, relative to L.

Experimental

The ligand L was synthesised according to literature procedures.^{9a} Trimethylphosphine was purchased from Aldrich Chemical Co. as a 1.0 mol dm⁻³ solution in toluene or as a pure liquid. Ethylene glycol monoethyl ether was dried by distillation before use. All other solvents and materials were of reagent quality and were used without further purification.

Measurements.—Elemental analyses were performed by

† Supplementary data available: see Instructions for Authors, *J. Chem. Soc., Dalton Trans.*, 1991, Issue 1, pp. xviii–xxii.

Table 1 Experimental data for the crystallographic study of *trans*-[RuL(Cl)(PMe₃)₂]ClO₄

Crystal data	
Empirical formula	C ₂₉ H ₃₅ Cl ₂ N ₅ O ₄ P ₂ Ru
Colour, habit	Ruby-red block
Crystal size (mm)	0.30 × 0.30 × 0.25
Crystal system	Trigonal
Space group	<i>P</i> 3 ₁ 21 (no. 152)
Unit-cell dimensions/Å	<i>a</i> = 14.158(2), <i>c</i> = 14.493(3)
<i>U</i> /Å ³	2515.8(9)
<i>Z</i>	3
<i>M</i>	751.5
<i>D_c</i> /Mg m ⁻³	1.488
<i>μ</i> /mm ⁻¹	0.752
<i>F</i> (000)	1152
Data collection	
Radiation	Mo-Kα (<i>λ</i> = 0.710 73 Å)
<i>T</i> /K	295
Monochromator	Highly oriented graphite
2θ Range/°	5.0–45.0
Scan type	2θ(counter)–θ(crystal)
Scan speed	Constant; 2.19° min ⁻¹ in ω
Scan range (ω)/°	0.65 plus Kα separation
Background measurement	Stationary crystal and stationary counter at beginning and end of scan, each for 25.0% of total scan time
Index ranges	0 ≤ <i>h</i> ≤ 15, –15 ≤ <i>k</i> ≤ 13, –15 ≤ <i>l</i> ≤ 15
Reflections collected	6963
Independent reflections	2221 (<i>R</i> _{int} = 0.0120)
Absorption correction	Empirical
Solution and refinement	
System used	Siemens SHELXTL PLUS (VMS) ²²
Refinement method	Full-matrix least squares
Quantity minimized	Σ(<i>w</i> (<i>F_o</i> – <i>F_c</i>) ²)
Extinction correction	<i>χ</i> = 0.000 07(7), where <i>F</i> * = <i>F</i> [1 + 0.002 <i>χF</i> ² /sin(2θ)] ^{-1/4}
Weighting scheme	<i>w</i> ⁻¹ = σ ² (<i>F</i>) + 0.0003 <i>F</i> ²
Number of parameters refined	212
Final <i>R</i> indices (all data)	<i>R</i> = 0.0283, <i>R</i> ' = 0.0267
(6σ data)	<i>R</i> = 0.0223, <i>R</i> ' = 0.0246 for those 1942 data with <i>F</i> > 6.0σ(<i>F</i>)
Goodness-of-fit	1.08
Data-to-parameter ratio	10.5:1
Largest difference peak/e Å ⁻³	0.49
Largest difference hole/e Å ⁻³	–0.30

Atlantic Microlabs (Norcross, GA). Proton NMR spectra were obtained using a Varian EM-390 90 MHz spectrometer, ¹³C NMR spectra with a JEOL FX-90Q FT spectrometer. All spectra were obtained using deuterated chloroform as the solvent, using SiMe₄ (¹H) and the centre line of the CDCl₃ resonance at δ 77.0 (¹³C) as references. The UV/VIS electronic spectra were obtained with a Bausch & Lomb Spectronic 2000 electronic spectrophotometer equipped with a Houston Instrument model 200 recorder or a Milton Roy Spectronic 3000 diode-array spectrophotometer equipped with a Hewlett-Packard 7470A plotter. Cyclic voltammetric measurements were obtained with an IBM EC/225 voltammetric analyser and the current–potential waves were recorded with a Houston Instruments model 100 X-Y recorder. These experiments were performed in a three-electrode, one-compartment cell, equipped with a platinum working electrode (Bioanalytical Systems), a platinum auxiliary electrode, and a saturated sodium chloride calomel electrode (SSCE) as the reference electrode. Electrochemical measurements in CH₂Cl₂ used 0.1 mol dm⁻³ tetrabutylammonium tetrafluoroborate as the supporting electrolyte. Magnetic susceptibility measurements

were accomplished with a Johnson Matthey magnetic susceptibility balance, using the Gouy method; the balance was calibrated using Hg[Co(SCN)₄].²⁰

Preparations.—[2,6-Bis(3-phenylpyrazol-1-yl)pyridine]-trichlororuthenium(III) monohydrate, [RuLCl₃]·H₂O **1**. A sample of RuCl₃·3H₂O (0.131 g, 5.0 × 10⁻⁴ mol) was mixed with ligand L (0.181 g, 1.0 equivalent) in ethylene glycol monoethyl ether (62.5 cm³). The solution was heated at reflux under nitrogen for 6 h. After cooling to room temperature, the black-green precipitate which formed was collected by vacuum filtration from a dark red filtrate. The solid was washed thoroughly with absolute EtOH and Et₂O and air dried. Yield of complex **1** 0.243 g, 85%. *E*_{1/2}(CH₂Cl₂) = –0.01 V, +1.46 V vs. SSCE. Effective magnetic moment (*μ*_{eff}) = 0.65 (Found: C, 46.7, H, 2.90. C₂₃H₁₇Cl₃N₅Ru·H₂O requires C, 46.9; H, 3.25%).

trans-[2,6-Bis(3-phenylpyrazol-1-yl)pyridine]dichloro(trimethylphosphine)ruthenium(II), *trans*-[RuLCl₂(PMe₃)]·1.25-CHCl₃ **2**. Complex **1** (0.056 g, 9.8 × 10⁻⁵ mol) was mixed with five drops of PMe₃ in CHCl₃ (15 cm³) in an inert-atmosphere glove-box. The mixture was taken outside the glove-box and triethylamine (2 cm³) was added as a reductant. The mixture was heated at reflux under nitrogen for 10 h. The resultant microcrystalline purple-brown solid was collected by vacuum filtration, washed with the minimum amount of absolute EtOH and Et₂O and air dried. Yield of complex **2** 0.059 g, 98%. UV/VIS (CH₂Cl₂): *λ*_{max} 495 (ε 3400), 364 (2900), 326 (14 700), 316 (sh) and 292 nm (19 300 dm³ mol⁻¹ cm⁻¹). *E*_{1/2}(CH₂Cl₂) = +0.41 V vs. SSCE (Found: C, 42.9; H, 3.5. C₂₆H₂₆Cl₂N₅P·Ru·H₂O·1.25CHCl₃ requires C, 43.0; H, 3.6%).

cis-[2,6-Bis(3-phenylpyrazol-1-yl)pyridine]dichloro(trimethylphosphine)ruthenium(II), *cis*-[RuLCl₂(PMe₃)]·CHCl₃ **3**. Complex **2** (0.051 g, 8.3 × 10⁻⁵ mol) was added to CHCl₃ (45 cm³) and irradiated under nitrogen for 61 h with a 120 W tungsten light. The solvent was then completely removed by rotary evaporation. The solid was slurried in CH₂Cl₂ (2 cm³) and then dropped into Et₂O (*ca.* 20 cm³). The light brown solid was collected by vacuum filtration. Yield of complex **3** 0.031 g, 61%. UV/VIS (CH₂Cl₂): *λ*_{max} 483 (ε 5200), 319 (19 200) and 292 nm (25 800 dm³ mol⁻¹ cm⁻¹). *E*_{1/2}(CH₂Cl₂) = +0.56 V vs. SSCE (Found: C, 44.7; H, 4.0%. C₂₆H₂₆Cl₂N₅PRu·CHCl₃ requires C, 44.4; H, 3.7%).

CAUTION. While the authors have used perchlorate as a counter ion with a number of ruthenium complexes without incident, perchlorate salts of metal complexes with organic ligands are potentially explosive. Care should be exercised in using a spatula or stirring rod mechanically to agitate any solid perchlorate. These complexes, as well as any other perchlorate salt, should only be handled in small quantities, using the appropriate safety procedures.²¹

trans-[2,6-Bis(3-phenylpyrazol-1-yl)pyridine]chlorobis(trimethylphosphine)ruthenium(II) perchlorate, *trans*-[RuL(Cl)(PMe₃)₂]ClO₄ **4**. Complex **1** (1.45 g, 2.6 × 10⁻³ mol) was added to CH₂Cl₂ (435 cm³) and degassed with N₂(g). A 1.0 mol dm⁻³ solution of PMe₃ (5.2 equivalents, 13 cm³) was quickly added by syringe to the ruthenium suspension followed by Zn/Hg amalgam (14.23 g). The mixture was heated at reflux under nitrogen for 24 h, then the heating mantle was removed from the brown suspension and the mixture was irradiated under a 120 W spotlight for 4 d. After the amalgam and some insoluble green solids had been filtered from the orange-brown mixture, the solvent was completely removed from the filtrate. The orange residue was dissolved in 95% EtOH (*ca.* 300 cm³) and the solution filtered to remove any insoluble materials. Solid NaClO₄ (3 g) was added and the volume slowly reduced to *ca.* 80 cm³ by the use of a rotary evaporator. The red-orange microcrystalline product was washed with the minimum amount of water and air dried. The solid was purified, if necessary, on a column of deactivated basic alumina (1 cm³ distilled water per 10 cm³ alumina), by dissolving in and eluting with acetone. The major yellow-orange band was collected, the

Table 2 Atomic coordinates ($\times 10^4$) for complex **4**

Atom	x	y	z
Ru	6 927(1)	6 927(1)	0
Cl(1)	5 214(1)	5 214(1)	0
P(1)	7 524(1)	6 193(1)	1 177(1)
C(1)	8 388(6)	5 677(6)	820(3)
C(2)	8 379(4)	7 183(5)	2 030(3)
C(3)	6 496(4)	5 130(4)	1 884(4)
N(11)	8 313(3)	8 313(3)	0
C(12)	8 436(3)	9 171(3)	502(3)
C(13)	9 390(3)	10 167(3)	511(3)
C(14)	10 255(4)	10 255(4)	0
N(21)	6 639(2)	7 838(2)	1 002(2)
N(22)	7 490(3)	8 909(2)	999(2)
C(23)	7 324(4)	9 511(4)	1 642(3)
C(24)	6 378(4)	8 846(4)	2 064(3)
C(25)	5 959(3)	7 810(3)	1 656(2)
C(31)	4 968(3)	6 801(3)	1 949(3)
C(32)	4 921(4)	6 474(5)	2 836(3)
C(33)	4 017(5)	5 558(5)	3 147(3)
C(34)	3 147(4)	4 971(5)	2 602(4)
C(35)	3 189(4)	5 289(4)	1 740(3)
C(36)	4 097(4)	6 217(4)	1 394(3)
Cl(2)	0	2 953(1)	1 667
O(1)	0	3 903(7)	1 667
O(2)	807(3)	2 843(3)	1 227(3)
O(3)	-500(14)	3 289(18)	1 011(13)
O(4)	-648(13)	2 498(12)	846(11)

Table 3 Bond lengths (\AA)

Ru-Cl(1)	2.426(1)	Ru-P(1)	2.363(1)
Ru-N(11)	1.962(4)	Ru-N(21)	2.112(3)
Ru-P(1A)	2.363(1)	Ru-N(21A)	2.112(3)
P(1)-C(1)	1.787(10)	P(1)-C(2)	1.805(5)
P(1)-C(3)	1.801(5)	N(11)-C(12)	1.351(4)
N(11)-C(12A)	1.351(4)	C(12)-C(13)	1.382(4)
C(12)-N(22)	1.397(5)	C(13)-C(14)	1.383(5)
C(14)-C(13A)	1.383(5)	N(21)-N(22)	1.388(3)
N(21)-C(23)	1.338(5)	N(22)-C(23)	1.360(6)
C(23)-C(24)	1.339(6)	C(24)-C(25)	1.408(6)
C(25)-C(31)	1.478(5)	C(31)-C(32)	1.357(6)
C(31)-C(36)	1.354(6)	C(32)-C(33)	1.365(7)
C(33)-C(34)	1.344(7)	C(34)-C(35)	1.319(8)
C(35)-C(36)	1.394(6)	Cl(2)-O(1)	1.345(11)
Cl(2)-O(2)	1.382(5)	Cl(2)-O(3)	1.404(24)
Cl(2)-O(4)	1.442(15)	Cl(2)-O(2A)	1.382(5)
Cl(2)-O(3A)	1.403(19)	Cl(2)-O(4A)	1.441(15)

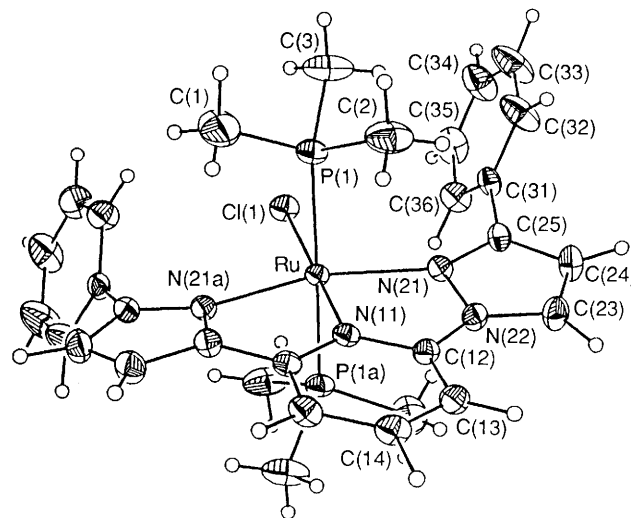
volume was reduced and the solid was triturated with Et_2O . Yield of complex **4** 1.32 g, 69.2%. UV/VIS (CH_2Cl_2): λ_{max} 434 (ϵ 6200), 320 (24 100) and 284 nm ($37\,700\text{ dm}^3\text{ mol}^{-1}\text{ cm}^{-1}$). NMR (90 MHz, CDCl_3): ^1H , δ 0.8 (18 H, t, $J = 3$, CH_3), 6.8 (2 H, d, $J = 3$, $\text{N}_2\text{C}_3\text{H}_2$), 7.3 [6 H, m, C_6H_5 (*m*- and *p*-H)], 7.6 [4 H, m, C_6H_5 (*o*-H)], 8.1 (3 H, s, NC_5H_3), 8.8 (2 H, d, $J = 3$ Hz, $\text{N}_2\text{C}_3\text{H}_2$) (T = second-order virtually coupled, 1:2:1 triplet); ^{13}C , δ 161.0, 150.0, 137.2, 132.4, 130.0, 128.2, 127.8, 122.2, 112.9, 107.3 and 12.4 (T). $E_{1/2}(\text{CH}_2\text{Cl}_2) = +0.94\text{ V vs. SSCE}$ (Found: C, 46.25; H, 4.7. $\text{C}_{29}\text{H}_{35}\text{Cl}_2\text{N}_5\text{O}_4\text{P}_2\text{Ru}$ requires C, 46.35; H, 4.7%).

Alternate procedure. Complex **3** (0.10 g, 1.6×10^{-4} mol) was mixed with seven drops of PMe_3 in acetone (40 cm^3) and EtOH (20 cm^3), in an inert-atmosphere glove-box. The mixture was brought out of the glove-box and stirred under nitrogen, in darkness, at room temperature, overnight. The solvent of the orange solution was completely removed using a rotary evaporator. The ClO_4^- salt was isolated and purified as above. Yield of complex **4** 0.069 g, 56%. Overall yield starting from **1** 33%.

X-Ray Data Collection.—Ruby-red crystals of *trans*- $[\text{RuL}(\text{Cl})(\text{PMe}_3)_2]^+\text{ClO}_4^-$ were prepared by slow vapour diffusion

Table 4 Bond angles ($^\circ$)

Cl(1)-Ru-P(1)	87.6(1)	Cl(1)-Ru-N(11)	180.0(1)
P(1)-Ru-N(11)	92.4(1)	Cl(1)-Ru-N(21)	102.0(1)
P(1)-Ru-N(21)	89.6(1)	N(11)-Ru-N(21)	78.0(1)
Cl(1)-Ru-P(1A)	87.6(1)	P(1)-Ru-P(1A)	175.3(1)
N(11)-Ru-P(1A)	92.4(1)	N(21)-Ru-P(1A)	91.4(1)
Cl(1)-Ru-N(21A)	102.0(1)	P(1)-Ru-N(21A)	91.4(1)
N(11)-Ru-N(21A)	78.0(1)	N(21)-Ru-N(21A)	156.0(1)
P(1A)-Ru-N(21A)	89.6(1)	Ru-P(1)-C(1)	116.1(2)
Ru-P(1)-C(2)	113.7(2)	C(1)-P(1)-C(2)	100.7(3)
Ru-P(1)-C(3)	117.5(2)	C(1)-P(1)-C(3)	104.8(3)
C(2)-P(1)-C(3)	102.0(2)	Ru-N(11)-C(12)	120.9(2)
Ru-N(11)-C(12A)	120.9(2)	C(12)-N(11)-C(12A)	118.1(4)
N(11)-C(12)-C(13)	122.9(4)	N(11)-C(12)-N(22)	111.3(3)
C(13)-C(12)-N(22)	125.8(4)	C(12)-C(13)-C(14)	117.2(4)
C(13)-C(14)-C(13A)	121.6(5)	Ru-N(21)-N(22)	109.8(2)
Ru-N(21)-C(25)	145.6(2)	N(22)-N(21)-C(25)	104.6(3)
C(12)-N(22)-N(21)	119.0(3)	C(12)-N(22)-C(23)	129.0(3)
N(21)-N(22)-C(23)	110.8(3)	N(22)-C(23)-C(24)	117.3(4)
C(23)-C(24)-C(25)	107.1(4)	N(21)-C(25)-C(24)	110.1(3)
N(21)-C(25)-C(31)	123.6(4)	C(24)-C(25)-C(31)	126.0(4)
C(25)-C(31)-C(32)	117.6(3)	C(25)-C(31)-C(36)	123.6(4)
C(32)-C(31)-C(36)	118.8(4)	C(31)-C(32)-C(33)	119.9(4)
C(32)-C(33)-C(34)	121.8(5)	C(33)-C(34)-C(35)	118.4(4)
C(34)-C(35)-C(36)	121.7(4)	C(31)-C(36)-C(35)	119.4(4)

**Fig. 1** A general view of the *trans*- $[\text{RuL}(\text{Cl})(\text{PMe}_3)_2]^+$ cation

from an acetone-cyclohexane solution. The crystal selected for the X-ray diffraction study was mounted on a four-circle diffractometer (Syntex $\text{P}2_1$ upgraded to Siemens $\text{P}3/\text{V}$); the resulting crystal data and other crystallographic details are reported in Table 1. Items of particular note are as follows. (1) Tests for absolute configuration show the space group of the crystal studied to be $\text{P}3_121$ rather than $\text{P}3_221$. (2) Hydrogen atoms were included in calculated positions based on $d(\text{C}-\text{H}) = 0.96\text{ \AA}$ and with $U = 0.08\text{ \AA}^2$. (3) The cation is ordered and lies about the two-fold axis at $\bar{x}, \bar{x}, 0$ (Wyckoff position *a*); the ClO_4^- anion is unpleasantly disordered about the two-fold axis at $0, x, \frac{1}{2}$ (Wyckoff position *b*). Nevertheless, the structure was well behaved and refinement (anisotropic for all non-hydrogen atoms) converged with $R = 0.0283$ for all data with $F > 6\sigma(F)$. Final atomic coordinates are listed in Table 2.

Additional material available from the Cambridge Crystallographic Data centre comprises H-atom coordinates and thermal parameters.

Results and Discussion

A general view of the $[\text{RuL}(\text{Cl})(\text{PMe}_3)_2]^+$ cation is shown in Fig. 1. The atoms defined in Table 1 are labelled normally; those

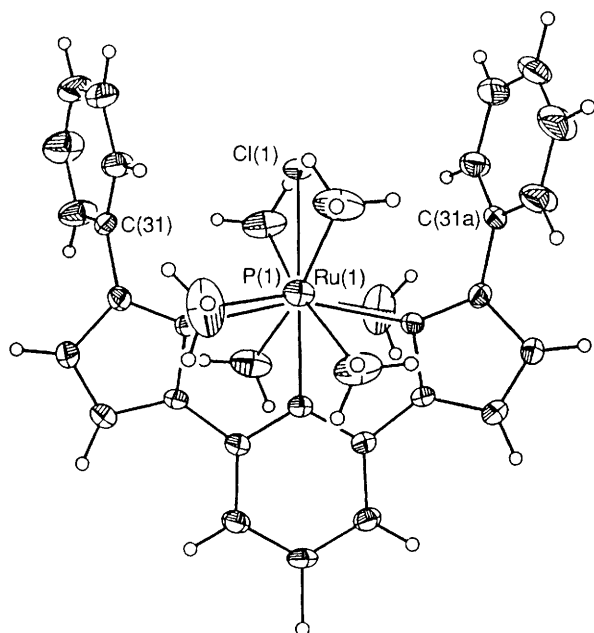


Fig. 2 The $trans\text{-}[\text{RuL}(\text{Cl})(\text{PMe}_3)_2]^+$ ion viewed with the C_2 axis vertical. Note the spreading of the outer phenyl groups away from the co-ordination sites in the vertical plane

related to the basic asymmetric unit by rotation about the C_2 axis (at $x, x, 0$) are given the suffix 'a'. Interatomic distances and angles are given in Tables 3 and 4.

The syntheses of the $\text{Ru}^{\text{III}}\text{L}(\text{PMe}_3)$ complexes follow the general syntheses reported for recent work with terpy with some exceptions.^{18,23} The initial chelation of L in the synthesis of complex **1** requires more forcing conditions than those required for the synthesis of $[\text{RuCl}_3(\text{terpy})]$. Thus, refluxing ethylene glycol monoethyl ether is used instead of refluxing MeOH or EtOH. The complexes utilizing L are less soluble than the analogous terpy complexes; this is advantageous as the former are often isolated from the reaction mixture without the need for further purification. However the conversion of $trans\text{-}$ into $cis\text{-}[\text{RuLCl}_2(\text{PMe}_3)]$ requires a much longer irradiation time than for similar terpy complexes, due to the insolubility of the complexes. Just as the synthesis of the analogous $trans\text{-}[\text{RuCl}(\text{terpy})(\text{PMe}_3)_2]\text{ClO}_4$ complex exhibits higher yields from the one-pot synthesis,¹⁸ so does that of the L complexes (an increase of 36% overall).

The $E_{1/2}$ values for the $\text{Ru}^{\text{III}}\text{-Ru}^{\text{II}}$ couples of the newly synthesised $\text{Ru}^{\text{III}}\text{L}(\text{phosphine})$ complexes are similar to those we reported for the analogous $\text{Ru}^{\text{III}}(\text{terpy})(\text{phosphine})$ complexes: $trans\text{-}[\text{RuCl}_2(\text{terpy})(\text{PMe}_3)]$ 0.41 V, $cis\text{-}[\text{RuCl}_2(\text{terpy})(\text{PMe}_3)]$ 0.57 V and $trans\text{-}[\text{RuCl}(\text{terpy})(\text{PMe}_3)_2]\text{ClO}_4$ 0.73 V vs. SSCE in CH_2Cl_2 . Only the $E_{1/2}$ values for $trans\text{-}[\text{RuL}(\text{Cl})(\text{PMe}_3)_2]\text{ClO}_4$ and $trans\text{-}[\text{RuCl}(\text{terpy})(\text{PMe}_3)_2]\text{ClO}_4$ show a significant difference in magnitude, differing by 210 mV.

The current methods of synthesising $trans\text{-}[\text{RuL}'(\text{Cl})(\text{PMe}_3)_2]\text{ClO}_4$ complexes (where $L' = \text{tridentate ligand}$) require the initial formation of $trans\text{-}[\text{RuL}'\text{Cl}_2(\text{PMe}_3)]$, where trimethylphosphine is bonded in the fourth meridional position of an octahedral ruthenium complex (the other meridional positions are occupied by the tridentate ligand).^{17,18,21} As noted above, the formation of $trans\text{-}[\text{RuLCl}_2(\text{PMe}_3)]^+$ proceeded smoothly, while we were unable to generate the analogous $trans\text{-}[\text{RuCl}_2(\text{dpt})(\text{PMe}_3)]^+$. Although L and dpt are quite similar in structure, we can rationalise the difference in the ease of synthesis of the L complex relative to the dpt complex by asserting that dpt exerts a much greater steric constraint on the fourth meridional site than does L.

In order to substantiate our claims regarding the steric

properties of dpt relative to L, we can utilise crystal-structure data to estimate the steric sizes of these ligands. Constable¹⁴ has observed that, to act as an efficient tridentate ligand, terpy must distort from ideal ligand geometry to reduce the interannular angle between the central and terminal pyridine rings. From the crystal structure of $trans\text{-}[\text{Ru}(\text{NO}_2)(\text{terpy})(\text{PMe}_3)_2]^+$ we have observed a similar distortion from the ideal geometry of terpy.^{18a} When the interannular angle is reduced in terpy the 6,6'' positions are directed towards the fourth meridional position. Although the crystal structure of a transition-metal dpt complex has not been reported, we can estimate the approximate interphenyl distance of the dpt ligand from the crystal structure of $trans\text{-}[\text{Ru}(\text{NO}_2)(\text{terpy})(\text{PMe}_3)_2]^+$ (phenyl rings must be inserted into 6,6'' positions of the terpy ligand). If we assume that an aromatic π cloud has a van der Waals thickness of 3.4 Å, the distance between the phenyl arms (interphenyl distance) for the fourth meridional site of the dpt complex should be ≈ 1.8 Å at a distance of ≈ 2.4 Å from the centre of the ruthenium. {The distance of ≈ 2.4 Å is the Ru-P bond length in $trans\text{-}[\text{RuL}(\text{Cl})(\text{PMe}_3)_2]^+$.} In a similar manner, we can estimate the approximate interphenyl distance of the ligand L from the crystal-structure data of complex **4**. The interphenyl distance for the fourth meridional site of the L complex is ≈ 4.2 Å at a distance of ≈ 2.4 Å from the centre of the ruthenium. Note that with L, the phenyl rings are directed away from the fourth meridional position (see Fig. 2).

By comparing the minimum van der Waals diameter of trimethylphosphine [≈ 5.6 Å, as calculated with Corey-Pauling-Koltun (CPK) models]^{24,25} with the interphenyl distance of L (≈ 4.2 Å) and dpt (≈ 1.8 Å), we would predict that neither ligand should be contained in a $trans\text{-}[\text{RuLCl}_2(\text{PMe}_3)]$ complex. However, in order to incorporate trimethylphosphine between the phenyl rings, we can assert that L would have to distort less from its observed crystallographic structure than dpt (as estimated from the terpy structure). Our ability to synthesise only $trans\text{-}[\text{RuLCl}_2(\text{PMe}_3)]$ **2** supports this contention.

A second way of assessing the steric constraint that the phenyl groups of dpt and L exert on the fourth meridional position is to evaluate the steric properties of the free ligands. We utilized CPK models²⁴ to represent the idealised geometries of the ligands because crystal structure data on either of the free dpt or L ligands are unavailable. For the free ligands, the interphenyl distance for L is ≈ 7.2 Å and for the dpt is ≈ 3.4 Å. The trimethylphosphine ligand (van der Waals diameter ≈ 5.6 Å) can readily fit between the phenyl groups of free L, but not between those of free dpt. In order for trimethylphosphine to fit between the phenyl groups of the dpt ligand the latter would have to be severely distorted from the idealised free-ligand configuration.

From both of our steric assessments, and from the fact that $trans\text{-}[\text{RuLCl}_2(\text{PMe}_3)]$ is synthetically accessible and $trans\text{-}[\text{RuCl}_2(\text{dpt})(\text{PMe}_3)]$ is not, we propose that for ruthenium(II) complexes the L and dpt ligands probably assume configurations ranging from our observed X-ray crystal structure configurations to those of the free-ligand configurations approximated by CPK models, depending on the steric constraints of the remaining ligands of the ruthenium(II) complexes.²⁵ We set the free-ligand configurations as the upper limit of distortion, due to the above-mentioned observations by Constable¹⁴ regarding terpy distortion from the free-ligand geometry.

Our failure to utilise dpt in our target ruthenium(II) complexes does not imply that dpt cannot be incorporated into ruthenium(II) complexes. For example, the $[\text{Ru}(\text{dpt})_2]^{2+}$ complex was synthesised by McMillin and co-workers,⁷ to examine the role of the phenyl substituent with regard to the excited-state lifetime of $[\text{Ru}(\text{dpt})_2]^{2+}$. However, it was observed that $[\text{Ru}(\text{dpt})_2]^{2+}$ displayed an unexpectedly large amount of photodecomposition. It was determined from molecular models

that interligand steric repulsions exist within the $[\text{Ru}(\text{dpt})_2]^{2+}$ complex between the phenyl substituents of one dpt ligand and the central pyridine ring of the second dpt ligand; the pyridine ring of the second dpt ligand occupies the fourth meridional position defined by the first dpt ligand. When $[\text{Ru}(\text{dpt})_2]^{2+}$ is irradiated in the presence of a co-ordinating anion (X) the excited-state complex responds to the steric repulsions of the dpt ligand by adopting a $[\text{Ru}(\text{dpt})(\text{dpt}')(\text{X})]^+$ configuration (where dpt' denotes the release of one of the phenylpyridine arms to form a bidentate terpy ligand).⁷ Thus, while the dpt ligand can co-ordinate to ruthenium(II), the size of the ligand co-ordinated within the phenyl arms can interfere with co-ordination of the dpt ligand.

Finally, the crystal structure of *trans*- $[\text{RuL}(\text{Cl})(\text{PMe}_3)_2]\text{ClO}_4$ yields some notable differences in the co-ordination of the ligand L when compared to terpy analogues. The bond angle of the central pyridine is C(12)–N(11)–C(12a) 118.1(4)°; this is significantly smaller than that observed for the central pyridine of the *trans*- $[\text{Ru}(\text{NO}_2)(\text{terpy})(\text{PMe}_3)_2]^+$ complex which has a bond angle of 122.1(5)°. This suggests the central pyridine (on the L ligand) is pulled inward toward the ruthenium centre to provide the central co-ordination site of the meridional ligand. The N(11)–C(12)–N(22) bond angle of 111.3(3)° is 4.9° smaller than the analogous bond angle in the terpy ligand in *trans*- $[\text{Ru}(\text{NO}_2)(\text{terpy})(\text{PMe}_3)_2]^+$. Likewise, the Ru–N(21)–N(22) bond angle of 109.8(2)° is 3.7° smaller and Ru–N(21)–C(25) 145.6(2)° is 16.7° larger than those of the terpy ligand in the *trans*- $[\text{Ru}(\text{NO}_2)(\text{terpy})(\text{PMe}_3)_2]^+$ complex. These changes in bond angles are consistent with the observation by Constable¹⁴ that the terpy ligand co-ordinates by an inward bending of the terminal pyridine groups, for the ligand L we observe less inward movement of the terminal pyrazoles when compared to terpy.

A comparison of the bond distances of *trans*- $[\text{RuL}(\text{Cl})(\text{PMe}_3)_2]^+$ against those of *trans*- $[\text{Ru}(\text{NO}_2)(\text{terpy})(\text{PMe}_3)_2]^+$ indicates the Ru–N (central N of ligand) bond length is smaller for the L complex by 0.023 Å while the equivalent Ru–N (pyrazoles of L) bond lengths are longer than those of the Ru–N (terminal pyridines of terpy) by 0.019–0.024 Å. The shorter length of the Ru–N (central pyridine) bond in the L complex (when compared to terpy), when complemented with the longer length of the Ru–N (pyrazole) bond distance (when compared to terpy), further corroborates the theory that the inward tilt of the terminal rings (or 'bite') of ligand L is lessened by the use of phenyl substituents.

The Ru–P bond lengths [2.363(1) Å] of *trans*- $[\text{RuL}(\text{Cl})(\text{PMe}_3)_2]^+$ are similar to those found in the *trans*- $[\text{Ru}(\text{NO}_2)(\text{terpy})(\text{PMe}_3)_2]^+$ (2.361 and 2.368 Å).^{18a} While the crystal structure confirmed the *trans* configuration of the two trimethylphosphine ligands, the P(1)–Ru–P(1a) bond angle of 175.3(1)° is less than expected for strictly octahedral co-ordination. The Ru–Cl(1) bond length of 2.426(1) Å may be compared with those found in such complexes as *trans*- $[\text{RuCl}(\text{Hdpg})_2(\text{NO})]$ (Hdpg = diphenylglyoximate) (2.309 Å),²⁶ $[\text{RuCl}_2(\text{MeC}_6\text{H}_4\text{CHMe}_2)(\text{PMePh}_2)]$ (2.414 Å),²⁷ and $[\text{Ru}(\text{CO})\text{Cl}_2(\text{PMe}_2\text{Ph})_2(\text{C}_2\text{H}_4)]$ (*trans* to CO, 2.454; *trans* to C₂H₄, 2.415 Å).²⁸ Thus, no significant strain is present in the bond of the phosphine ligand nor in the co-ordination of the chloride ligand due to the use of the ligand L.

Acknowledgements

This work was supported in part by the National Science Foundation (CHE 8814638), the donors of the Petroleum Research Fund, administered by the American Chemical

Society, the Whitaker Foundation of the Research Corp., Gettysburg College through an Institutional Self Renewal Grant, and the ARCO Chemical Co. Upgrade of the diffractometer was made possible by Grant 89-13733 from the Chemical Instrumentation Program of the National Science Foundation. We also acknowledge Johnson Matthey plc for a generous loan of $\text{RuCl}_3 \cdot 3\text{H}_2\text{O}$.

References

- 1 A. Skorbogaty and T. D. Smith, *Coord. Chem. Rev.*, 1984, **53**, 55.
- 2 R. C. Young, J. K. Nagle, T. J. Meyer and D. G. Whitten, *J. Am. Chem. Soc.*, 1978, **100**, 4773.
- 3 J.-P. Collin, S. Guillerez and J.-P. Sauvage, *J. Chem. Soc., Chem. Commun.*, 1989, 776.
- 4 A. Llobet, P. Doppelt and T. J. Meyer, *Inorg. Chem.*, 1988, **27**, 514; K. T. Potts, P. A. Usifer, A. Guadalupe and H. D. Abruna, *J. Am. Chem. Soc.*, 1987, **109**, 3961.
- 5 M. S. Thompson and T. J. Meyer, *J. Am. Chem. Soc.*, 1982, **104**, 5070.
- 6 C. C. Phifer and D. R. McMillin, *Inorg. Chem.*, 1986, **25**, 1329.
- 7 J. R. Kirchoff, D. R. McMillin, P. A. Marnot and J.-P. Sauvage, *J. Am. Chem. Soc.*, 1985, **107**, 1138 and refs. therein.
- 8 J. P. Collin and J.-P. Sauvage, *Inorg. Chem.*, 1986, **25**, 135.
- 9 (a) D. L. Jameson and K. A. Goldsby, *J. Org. Chem.*, 1990, **55**, 4992; (b) D. L. Jameson, J. K. Blaho, K. T. Kruger and K. A. Goldsby, *Inorg. Chem.*, 1989, **28**, 4312.
- 10 J. M. Veal and R. L. Rill, *Biochemistry*, 1988, **27**, 1822; C. O. Dietrich-Buchecker, P. A. Marnot, J.-P. Sauvage, J. R. Kirchoff and D. R. McMillin, *J. Chem. Soc., Chem. Commun.*, 1983, 513.
- 11 (a) P. A. Marnot, R. R. Ruppert and J.-P. Sauvage, *Nouv. J. Chim.*, 1981, **5**, 543; (b) C. L. Bailey and R. S. Drago, *J. Chem. Soc., Chem. Commun.*, 1987, 179.
- 12 T. J. Meyer, *Acc. Chem. Res.*, 1978, **11**, 94; R. D. Gillard, *Coord. Chem. Rev.*, 1983, **50**, 303.
- 13 A. Juris, V. Balzani, F. Barigelletti and S. Campagna, *Coord. Chem. Rev.*, 1988, **84**, 85 and refs. therein.
- 14 E. C. Constable, *Adv. Inorg. Chem. Radiochem.*, 1986, **30**, 69 and refs. therein.
- 15 C. O. Dietrich-Buchecker, P. A. Marnot, J.-P. Sauvage, J. P. Kintinger and P. Maltese, *Nouv. J. Chim.*, 1984, **8**, 573; J. R. Kirchoff, D. R. McMillin, P. A. Marnot and J.-P. Sauvage, *J. Am. Chem. Soc.*, 1985, **107**, 1138.
- 16 G. Sprintschnik, H. W. Sprintschnik, P. P. Kirsch and D. G. Whitten, *J. Am. Chem. Soc.*, 1977, **99**, 4947.
- 17 R. A. Leising and K. J. Takeuchi, *J. Am. Chem. Soc.*, 1988, **110**, 4079.
- 18 (a) R. A. Leising, S. A. Kubow, M. R. Churchill, L. A. Buttrey, J. W. Ziller and K. J. Takeuchi, *Inorg. Chem.*, 1990, **29**, 1306; (b) R. A. Leising, S. A. Kubow and K. J. Takeuchi, *Inorg. Chem.*, 1990, **29**, 4569.
- 19 (a) F. Krohnke, *Synthesis*, 1976, 1; (b) C. O. Dietrich-Buchecker, P. A. Marnot and J.-P. Sauvage, *Tetrahedron Lett.*, 1983, 5291.
- 20 B. N. Figgis and R. S. Nyholm, *J. Chem. Soc.*, 1958, 4190.
- 21 W. C. Wosley, *J. Chem. Educ.*, 1973, **50**, A335; K. Raymond, *Chem. Eng. News*, 1983, **61**, 4.
- 22 SHELXTL PLUS Program Set, Siemens, Analytical X-Ray Instruments Inc., Madison, WI, 1989.
- 23 B. P. Sullivan, J. M. Calvert and T. J. Meyer, *Inorg. Chem.*, 1980, **19**, 1404.
- 24 See R. A. Harte, *Molecules in Three Dimensions*, American Society of Biological Chemists, Bethesda, MD, 1969.
- 25 G. Ferguson, P. J. Roberts, E. C. Alyea and M. Khan, *Inorg. Chem.*, 1978, **10**, 2965.
- 26 L. F. Szczepura, J. G. Muller, C. A. Bessel, R. F. See, T. S. Janik, M. R. Churchill and K. J. Takeuchi, in preparation.
- 27 L. D. Brown, C. F. J. Barnard, J. A. Daniels, R. J. Mawby and J. A. Ibers, *Inorg. Chem.*, 1978, **17**, 2932.
- 28 M. A. Bennett, G. B. Robertson and A. K. Smith, *J. Organomet. Chem.*, 1972, **43**, C41.

Received 6th March 1991; Paper 1/01064F